9140 *Biochemistry* **2010,** *49,* 9140–9151
DOI: 10.1021/bi1004427

BIOCHEMISTRY
including biophysical chemistry & molecular biology
Article

Acetylation of GAGA Factor Modulates Its Interaction with DNA†

Xavier Aran-Guiu,‡ Miguel Ortiz-Lombardía,§ Eliandre Oliveira,∥ Carles Bonet Costa,‡ Maria Antonia Odena,∥ David Bellido,⊥ and Jordi Bernués*,‡

‡*Institut de Biologia Molecular de Barcelona-CSIC and Institute for Research in Biomedicine Barcelona, Parc Científic de Barcelona, Baldiri Reixac 10-12, 08028 Barcelona, Spain,* §*Architecture et Fonction des Macromolécules Biologiques* (*UMR6098*) *CNRS, Universités d'Aix-Marseille I & II, Marseille, France,* ∥*Plataforma de Proteòmica, Parc Científic de Barcelona, Barcelona, Spain, and* ⊥*Plataforma de Proteòmica, Parc Científic de Barcelona, Serveis Cientificotècnics, Universitat de Barcelona, Barcelona, Spain*

Received March 24, 2010; Revised Manuscript Received September 16, 2010

ABSTRACT: GAGA is a *Drosophila* transcription factor that shows a high degree of post-translational modification. Here, we show that GAGA factor is acetylated in vivo. Lysine residues K325 and K373 on basic regions BR1 and BR3 of the DNA binding domain, respectively, are shown to be acetylated by PCAF. While BR1 is strictly required to stabilize DNA binding, BR3 is dispensable. However, acetylation of both lysine residues, either alone or in combination, weakens the binding to DNA. Despite the high degree of conservation of K325 and K373 in flies, their mutation to glutamine does not affect DNA binding. Molecular dynamics simulations, using acetylated K325 and a K325Q mutant of GAGA DNA binding domain in complex with DNA, are fully consistent with these results and provide a thermodynamic explanation for this observation. We propose that while K325 and K373 are not essential for DNA binding they have been largely conserved for regulatory purposes, thus highlighting a key regulatory system for GAGA factor in flies.

The regulation of transcription is a crucial process in gene expression. For this purpose, cells make use of diverse mechanisms. Among these, post-translational modification (PTM)[1] has been intensively studied in the chromatin research field. In particular, since the proposal of the provocative histone code hypothesis (*1*), the PTM of histones has received much attention. Consequently, extensive knowledge of histone modifications has boosted interest in epigenetics. However, while some PTMs have been described for transcription factors, much less is known about their mapping and functions. A notable exception is p53, for which many PTMs have been shown to serve different functional roles (*2*, *3*).

Transcription factors are phosphorylated, acetylated, glycosylated, sumoylated, ubiquitinated, methylated, etc., in vivo, and in some cases, these modifications have been correlated with distinct functional states. While phosphorylation is the most studied PTM to date, acetylation and methylation are currently receiving much attention. In this respect, GAGA factor is remarkably modified in vivo (*4*). GAGA is a *Drosophila* transcription factor encoded in the single-copy gene *Trithorax-like* (*5*). GAGA factor is genetically classified in the Trithorax group of genes, which, in contrast to the action of the Polycomb group, maintain large regions of chromatin open to expression.

GAGA factor is remarkably complex, acting as a transcriptional activator and repressor, and also in the insulator function, chromatin remodeling, and position effect variegation, among others (*6*−*8*). In addition to possibly being O-glycosylated (*9*), GAGA factor can be phosphorylated in the proximity of the zinc finger of its DNA binding domain. This phosphorylation weakens its specific interaction with DNA (*4*). These experiments also demonstrated the presence of additional modifications in GAGA factor to explain the complex isoform protein pattern observed in two-dimensional (2D) gel electrophoresis. Here, we show that GAGA factor is also acetylated in vivo, and we analyze the functional consequences of this modification.

MATERIALS AND METHODS

Recombinant Proteins, Mutants, and Peptides. $GAGA_{519}$ and GAGADBD (residues 310−392) (*10*) were expressed as six-His-tagged proteins using pET14b (Novagen). 6xHis-SirT2, in the pET30c expression plasmid, was kindly provided by A. Vaquero (*11*). His-tagged fusion proteins were expressed in *Escherichia coli* BL21-DE3, purified using a HisTrap column (GE), and dialyzed against 100 mM KCl, 20% glycerol, 50 mM Hepes (pH 7.8), 0.5 mM EDTA, 0.5 mM DTT, and 0.2 mM PMSF. The HAT domain of human PCAF (residues 352−658) (in pGEX-2TK) (*12*) was expressed in *E. coli* BL21-DE3, purified on glutathione-Sepharose beads, and resuspended in acetylation buffer. Flag-tagged proteins HDAC1 (in pcDNA3) and HDAC2 (in pME18S) were expressed in transiently transfected HeLa cells as described previously (*13*) and then extracted and purified by immunoprecipitation using the M2 anti-Flag antibody (Sigma).

†X.A.-G. was supported in part by predoctoral fellowships FPI (from the CIRIT of the Generalitat de Catalunya) and I3P (from CSIC). The proteomics work was performed at the Proteomics Platform of Barcelona Science Park, University of Barcelona, a member of the ProteoRed network. This work was financed by Ministerio de Ciencia e Innovación of the Spanish Government Grants BFU2006-09761 and BFU2007-64395/BMC to J.B., and it was performed in the frame of the "Centre de Referència en Biotecnologia" of the Generalitat de Catalunya.

*To whom correspondence should be addressed: Institut de Biologia Molecular de Barcelona-CSIC and Institute for Research in Biomedicine Barcelona, Parc Científic de Barcelona, Baldiri Reixac 10-12, 08028 barcelona, Spain. E-mail: jordi.bernues@ibmb.csic.es. Phone: +34 934034960. Fax: +34 934034979.

[1]Abbreviations: GAGADBD, GAGA factor DNA binding domain; BR, basic regions; PTM, post-translational modification; MD, molecular dynamics.

 Published on Web 09/17/2010

Mutants in the DNA binding domain introducing either a Lys-325 → Gln change in the BR1 region (K325Q), a Lys-373 → Gln change in the BR3 region (K373Q), or both changes (Double) were prepared using the QuickChange II site-directed mutagenesis kit (Stratagene) in pET14b for later use in electrophoretic mobility shift assays (EMSAs) and in Act5PPA-GAGA$_{519}$ to generate the full-length mutants for transient transfection experiments.

Synthetic peptides BR1BR2 (STPKAKRAKHPPGTEKPRSRSQS) and BR3 (LRHFAKPGVKKEKKSKSGN) were obtained from Sigma Genosys as lyophilized powder and were resuspended in 0.1% acetic acid to a final concentration of 5 mg/mL.

Acetylation−Deacetylation Reactions. Proteins and peptides were acetylated as described previously (*14*), with either nonradioactive acetyl-CoA or [^{14}C]acetyl-CoA [1.85 GBq/mmol (NEN)] in 50 μL reaction mixtures containing 50 mM Tris-HCl (pH 8), 150 mM KCl, 0.5% NP-40, 5 mM EDTA, 40 ng of HAT enzyme, and 5 μg of chicken erythrocyte histones, 5 μg of synthetic peptides, or 5 μg of recombinant GAGADBD. Reaction mixtures were incubated at 30 °C for either 3 h or overnight.

Acetylated substrates and purified extracts from the *Drosophila* S2 cell line were deacetylated as described previously (*15*, *16*). NAD-dependent deacetylations were conducted in 25 μL reaction mixtures containing 0.5 mM NAD, 50 mM sodium phosphate (pH 7.2), 0.5 mM DTT, 50 ng of SirT2, and 20 μL of acetylation mixture or purified S2 extract (prepared as described above and dialyzed against deacetylation buffer) as the substrate. NAD-independent deacetylations were conducted in 25 μL reaction mixtures including 20 μL of acetylated recombinant GAGADBD and 50 ng of HDAC1 or HDAC2. In both cases, reaction mixtures were incubated at 37 °C for increasing times. Proteins were resolved on sodium dodecyl sulfate (SDS)−polyacrylamide gels, transferred to nitocellulose membranes (Optitran BA-S 85, Whatman), and exposed to Biomax MS film (Kodak) at −80 °C for 24 h.

Two-Dimensional Gel Electrophoresis. Crude nuclear extracts from wild-type *Drosophila* S2 cells were prepared as described previously (*4*, *17*). Extracts were fractionated through a phosphocellulose P11 ion exchange column. Fractions enriched with GAGA factor were pooled and precipitated with the 2D Clean-up kit (GEH). They were then resuspended in 8 M urea, 2% (w/v) Chaps, and 0.5% IPG buffer (pH 3−10) (GEH) and processed as described previously (*4*). Isoelectrofocusing was performed in an IPGphor Focusing System (GEH). Samples were loaded into Immobiline DryStrip pH 3−10 (GEH) preformed polyacrylamide strips (18 cm) and then hydrated for 6 h at 20 °C and prerun at 50 V for 8 h. Electrophoresis was performed for 2 h at 500 V, a gradient step of 6 h up to 1000 V, another gradient step of 3 h up to 8000 V, and a final step at 8000 V for 4 h. Strips were then equilibrated as described previously (*4*), and two-dimensional electrophoresis was performed on SDS−8% polyacrylamide gels. Proteins separated on gels were analyzed by Western blotting using an anti-GAGA antiserum.

Protein or Peptide Digestion. Prior to digestion, proteins were reduced with 10 mM dithiothreitol (DTT) and 50 mM Tris-HCl (pH 8) for 1 h at 56 °C and then alkylated with 55 mM iodoacetamide for 45 min in the dark. Proteins and synthetic peptides were digested with either trypsin (sequencing grade modified, Promega), V8 proteinase (endoproteinase Glu-C from *Staphylococcus aureus* strain V8, Sigma), or Arg-C endoproteinase (Sigma) following the manufacturer's specifications. The resulting peptides were concentrated and desalted using a microtip (ZipTipC18, Millipore). They were then washed with 0.1% trifluoroacetic acid (TFA) and eluted in a 2 mg/mL α-cyano-4-hydroxycinnamic acid matrix (Sigma) in 50% acetonitrile in 0.1% TFA on a MALDI plate and air-dried before analysis by mass spectrometry (dried droplet method).

Acquisition of MALDI-MS and MS/MS Spectra. Spectra were recorded in a MALDI-TOF/TOF 4700 Proteomics Analyzer (Applied Biosystems) with a 355 nm PowerChip Nano-Laser, operating at convenience, either in linear positive mode (for intact proteins) or in reflector positive mode (for digested peptides; voltage of 20 kV in source 1 and a laser intensity of ∼5400). Typically, 500 shots per spectrum were accumulated. MS/MS spectra were recorded using collision-induced dissociation (CID) with atmospheric air as the collision gas. An MS/MS 1 kV positive mode was used (voltage of 8 kV in source 1 and 15 kV in source 2).

EMSA Experiments. The ^{32}P-labeled d(CT·GA)$_5$ probe was prepared as described previously (*18*). One-half nanogram of labeled DNA fragment per reaction mixture was incubated with increasing amounts of GAGADBD, either acetylated or not, in the presence of 2.5 μg of bovine serum albumin and 50 ng of *E. coli* DNA, in 50 mM KCl, 15 mM Tris-HCl (pH 7.5), 0.1 mM EGTA, 0.5 mM DTT, and 6% glycerol, for 30 min at room temperature. After incubation, samples were loaded on a nondenaturing 4.5% polyacrylamide gel in 0.5× TBE buffer. After electrophoresis, gels were dried and exposed to autoradiographic film or to a storage phosphor screen (Molecular Dynamics) and quantified using ImageQuant version 5.2 (Molecular Dynamics). Binding was estimated as $1 - [(DNA_F/DNA_T)/(DNA_{F_0}/DNA_{T_0})]$, where DNA_T is the total amount of DNA loaded in each lane, DNA_F is the amount of free DNA fragment in the same lane, and DNA_{F_0}/DNA_{T_0} is the binding ratio in the lane without GAGADBD.

Transient Transfection Experiments. S2 cells were grown and transfected following standard procedures. Luciferase and β-galactosidase activities were then measured as described previously (*19*, *20*). Results were normalized as the ratio of enzymatic activities and are the average of at least three independent experiments performed in duplicate. Relative fold activation was calculated with respect to the relative activity of control cells transfected with the empty ActPPA expression vector (no GAGA overexpression) for each experiment. Even-skipped stripe 2-pGL3 and Trithorax-like-pGL3 constructs were used to monitor the activation and repression driven by GAGA factor, respectively, and CMV-βGal was used for normalization as described previously (*19*).

Molecular Dynamics Simulations. The calculations described in this study were conducted using the parm99 force field described by Cornell et al. (*21*), as implemented within the AMBER 9 suite of programs (*22*). The coordinates of the GAGA DNA binding domain (GAGADBD) in complex with DNA were taken from its solution structure, as determined by NMR spectroscopy, and deposited in the Protein Data Bank as entry 1YUI (*23*). The modified acetyllysine (acK325) residue was assigned RESP (*24*) charges consistent with the selected force field via the RED program, version III (*25*), using the multiconformation/multiorientation method (*26*). The geometrical parameters of acK325 were prepared with the LEaP module from AMBER version 9.0 (*27*). The nonbonded parameters for Zn^{2+} were taken from ref *28*. The seven following starting structures were prepared for the simulations: wild-type

GAGADBD−DNA, acK325 GAGADBD−DNA, and K325Q GAGADBD−DNA complexes, along with their four separate isolated constituents. The LEaP module from AMBER version 9 was used to cap the GAGADBD peptides with NME and ACE residues. LEaP was also used to attain electroneutrality via addition of appropriate ions and to place each starting structure into a truncated-octahedral periodic box of TIP3P water molecules. The distance between the edges of the water boxes and the closest atom of the solute was at least 12 Å.

The particle mesh Ewald (PME) method (*29*) was used to treat long-range electrostatic interactions, and bond lengths involving bonds to hydrogen atoms were constrained using SHAKE (*30*). The time step for MD simulations up to the equilibration was 2 fs, then 1 fs during the production runs. A direct-space nonbonded cutoff of 8 Å was used. The energy of the systems was minimized by 500 steps of steepest descent minimization followed by up to 500 steps of conjugate gradient minimization. Harmonic restraints with force constants of 2 kcal mol^{-1} Å^{-2} were applied to all solute atoms during the minimization. These restraints were maintained through a 50 ps canonical ensemble (NVT)-MD simulation, during which the systems were heated from 0 to 300 K. The restraints were also kept for a subsequent 50 ps isothermal isobaric ensemble (NPT)-MD, to adjust the solvent density. Finally, after unrestrained simulation for an additional 2 ns at 300 K with a time constant of 1.0 ps for heat-bath coupling, the following 20 ns was used to extract the snapshots for binding free energy calculations and free energy decomposition.

Energetic Analysis. The protein−DNA binding free energy can be expressed as

$$\Delta G_{\text{bind}} = \langle G_{\text{complex}} \rangle - \langle G_{\text{protein}} \rangle - \langle G_{\text{DNA}} \rangle$$

where the brackets denote averages over snapshots from independent MD trajectories. The free energy, G, for each species can be calculated by the following scheme using the MM-PBSA method:

$$G = E_{\text{gas}} + G_{\text{sol}} - TS$$

$$E_{\text{gas}} = E_{\text{int}} + E_{\text{ele}} + E_{\text{vdw}} + E_{\text{rot/trans}}$$

$$E_{\text{int}} = E_{\text{bond}} + E_{\text{angle}} + E_{\text{torsion}}$$

$$G_{\text{sol}} = G_{\text{PB}} + G_{\text{np}}$$

$$G_{\text{np}} = \gamma \text{SAS}$$

In this decomposition of energies, E_{gas} is the gas-phase energy, G_{sol} is the solvation free energy, and T and S are the temperature and the total solute entropy, respectively. E_{int} is the internal energy; E_{bond}, E_{angle}, and E_{torsion} are the bond, angle, and torsion energies, respectively. $E_{\text{rot/trans}}$ is the energy caused by six rotational and translational degrees of freedom, which in the classical limit amounts to $3RT$. E_{ele} and E_{vdw} are the Coulomb and van der Waals energies, respectively.

E_{gas} was calculated using the parm99 molecular mechanics force field described by Cornell et al. (*21*). G_{sol} can be decomposed into polar and nonpolar contributions. G_{PB} is the polar contribution of solvation calculated by solving the Poisson−Boltzmann equation, which was calculated with the pbsa program from AMBER version 9. The dielectric constants for solute and solvent were set at 1 and 80, respectively, and the ionic strength was set at 150 mM. The nonpolar solvation contribution (G_{np}) was estimated from the solvent accessible surface area (SAS) (*31*) determined using a water probe radius of 1.4 Å. The surface tension constant g was set at 0.0072 kcal mol^{-1} Å^{-2}. Vibrational, rotational, and translational entropy contributions were estimated by classical statistical thermodynamics, using normal-mode analysis. To obtain the normal modes, we minimized each snapshot in the gas phase using the conjugate gradient method with a distance-dependent dielectric constant of $4r$ (where r is the interatomic distance), until the root-mean-square deviation (rmsd) of the elements of the gradient vector was less than 5−10 kcal mol^{-1} Å^{-1}. All these calculations were performed using the mm_pbsa.pl script in AMBER version 9. The binding affinity was approximated from separate simulations of each complex and of their protein and DNA constituents. Snapshots taken every 20 ps from the 20 ns of production-phase simulation were evaluated for a total of 1500 structures per analyzed complex.

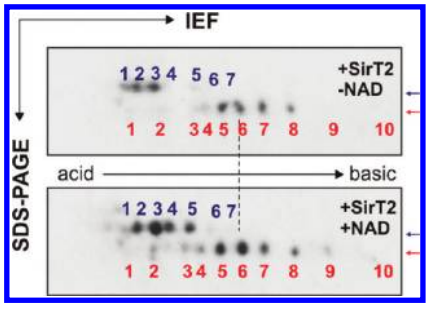

FIGURE 1: GAGA factor is acetylated in vivo. Two-dimensional gel electrophoresis of partially fractionated nuclear extracts from *Drosophila* S2 cells treated with SirT2 deacetylase in the absence and presence of NAD$^+$, as described in Materials and Methods (top and bottom panels, respectively). GAGA factor spots are revealed by Western blotting using specific antibodies. Arrows indicate spots for GAGA$_{519}$ and its presumably glycosylated form. The vertical dashed line between the number 6 spots is introduced to facilitate comparison.

RESULTS

GAGA Factor Is Acetylated in Vivo. GAGA factor is heavily modified in vivo (*4*). Two-dimensional (2D) gel electrophoresis of nuclear extracts enriched in GAGA factor from *Drosophila* S2 cells provided the first indication that, in addition to being phosphorylated, GAGA$_{519}$ was also acetylated in vivo. The GAGA$_{519}$ isoform resolves in 2D gels into numerous spots that are variable from sample to sample (possibly because of the biochemical fractionation schemes followed to enrich samples with GAGA factor). However, a pattern corresponding to two bands with slightly different apparent molecular masses (arrows in Figure 1), each containing several spots, was consistently obtained. The upper band might correspond to the glycosylated form because of its lower mobility, as reported previously (*17*) (not determined). In our extracts, the GAGA$_{581}$ isoform was not visible in 2D gels because it was less abundant than the GAGA$_{519}$ isoform in S2 cells. When the same sample was split in two and treated with SirT2 deacetylase in the absence and presence of NAD$^+$ (Figure 1, top and bottom panels, respectively), the 2D gel pattern of GAGA spots shifted to the right (to more basic pI values) after deacetylation, as expected. The two GAGA isoforms were only partially deacetylated by treatment of extracts with purified recombinant SirT2 deacetylase, in vitro, prior to

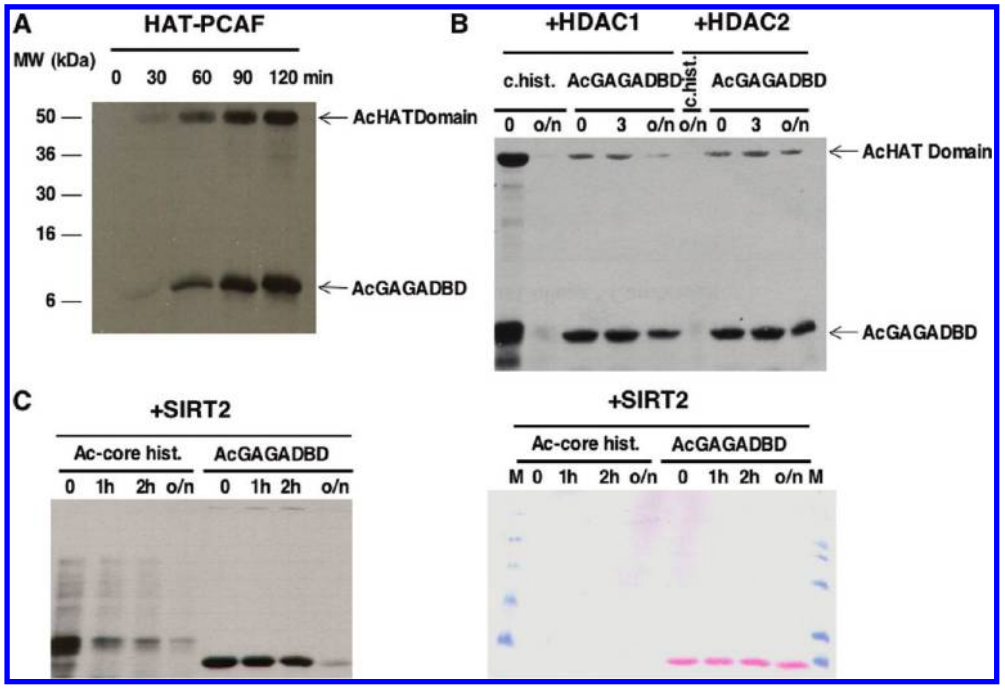

FIGURE 2: Recombinant GAGADBD is acetylated in vitro by HAT-PCAF and deacetylated by SirT2. (A) Kinetics of GAGADBD acetylation by recombinant HAT-PCAF in vitro. Autoacetylation of HAT-PCAF is indicated and serves as an internal control. (B) HAT-PCAF-acetylated GAGADBD is not deacetylated by HDAC1 (lanes 3−5) or by HDAC2 (lanes 7−9). Lanes 1, 2, and 6 show acetylated core histones either untreated or deacetylated by HDAC1 and HDAC2, respectively. (C) GAGADBD acetylated by HAT-PCAF is deacetylated by SirT2 much like acetylated core histones (autoradiograph in the left panel, lanes 5−8 and 1−4, respectively). The right panel shows a Ponceau stain of the same membrane.

electrophoresis. In fact, changes were more evident for the upper band. These gels suggested that more than one acetylation occurs because several spots changed distribution after deacetylation. Alternatively, a single acetylation might occur simultaneously with other PTMs that affect net pI (like phosphorylation). Attempts to further characterize the acetylation of GAGA factor by direct MS analysis of highly purified GAGA factor from S2 cells were not conclusive. Therefore, a more indirect approach was followed. Because of the nuclear localization and the high degree of conservation presented by this transcription factor, we used the well-known acetylase PCAF to acetylate recombinant GAGA factor in vitro. In fact, PCAF is the major histone H3 K9 and K14 acetyltransferase in flies (*32*). Initial experiments showed that GAGA was efficiently acetylated by HAT-PCAF in vitro, and while a minor signal was observed in the X domain, most of the signal was present in the region between residues 310 and 390, which encompass the DNA binding domain (results not shown). Acetylation was highly efficient and reached a plateau after 2 h (Figure 2A). In contrast, deacetylation was much more inefficient, and neither HDAC1 nor HDAC2 removed acetylation from GAGADBD. As a control, both enzymatic preparations were shown to efficiently remove acetylation from core histones similarly modified by HAT-PCAF (Figure 2B). Finally, recombinant SirT2 deacetylase efficiently removed acetylation from AcGAGADBD as well as from acetylated core histones in an overnight reaction (~16 h) (Figure 2C; the right panel shows a Ponceau staining of the membrane shown in the left panel to show similar protein loadings).

GAGA Factor Is Acetylated Mainly at the DNA Binding Domain. In addition to the unmodified peak, MALDI-TOF analysis of the acetylated form of GAGADBD revealed the presence of two main peaks (in Figure 3, compare panels A and B). These peaks, with mass increases of ~42 and ~84 Da, were

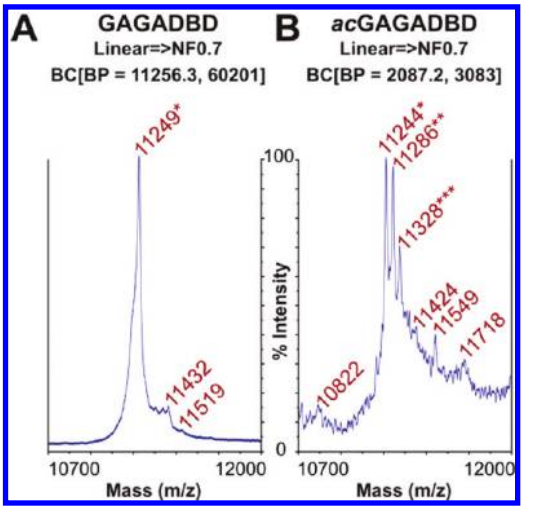

FIGURE 3: HAT-PCAF can acetylate GAGADBD at least at two different sites. MS spectra of nonacetylated (A) and acetylated (B) GAGADBD. Asterisks indicate unmodified (one), monoacetylated (two), and diacetylated (three) GAGADBD.

compatible with mono- and diacetylated forms, respectively. The spectra of the acetylated form also showed other minor peaks, which, in one case, might be compatible with the presence of a triacetylated form of GAGADBD. Because of the extremely low abundance of this potential tertiary acetylation site, it was not further studied.

Because GAGADBD is rich in lysine residues, routine trypsin digestion did not produce convenient peptides for further mapping of the modification by MS/MS. Therefore, an experimental approach using V8 protease digestion was set up to better define the residues modified. V8 protease cleaved GAGADBD at the acidic residues (mainly aspartates) present in this domain and,

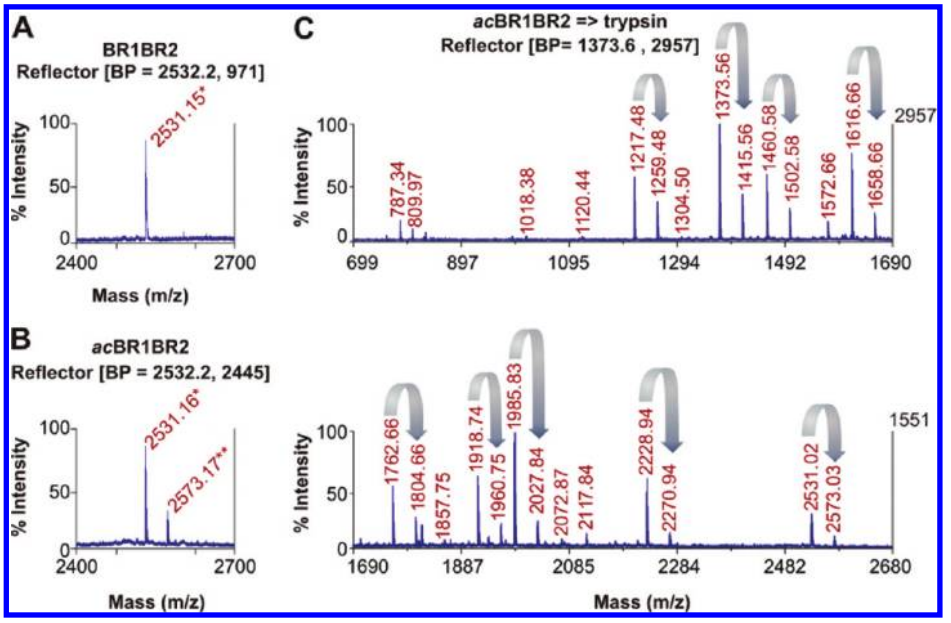

FIGURE 4: Basic region 1 of GAGADBD is acetylated by HAT-PCAF. Mass spectra of nonacetylated (labeled with an asterisk) (A) and acetylated BR1BR2 (labeled with two asterisks) (B). (C) Mass spectrum of acetylated BR1BR2 digested with trypsin (see Materials and Methods). Arrows indicate several pairs of acetylated/nonacetylated peptides. The spectrum is split in two halves for the sake of convenience.

under our experimental conditions, generated only two peptides that contained lysine residues. Gel electrophoresis and autoradiography showed that these peptides were acetylated, and this observation was confirmed by MALDI-TOF analysis (not shown). However, after MS/MS fragmentation, the small amount and length of these peptides did not allow unambiguous assignment of the residues modified. Nevertheless, these results restricted the acetylation sites to two regions: one encompassing basic regions 1 and 2 (BR1 and BR2, respectively) and the other comprising basic region 3 (BR3). Two peptides containing all the lysine residues of these regions were synthesized and assayed for acetylation as described above. The peptide encompassing BR1 and BR2 was efficiently acetylated in vitro (Figure 4). A clear acetylation was observed, as shown by an increase in the molecular mass of ~42 Da (compare nonacetylated and acetylated MALDI-TOF spectra in panels A and B, respectively). However, although a second acetylation was also detectable at this point, we could not analyze it further because of its very low abundance (not shown). Limited trypsin digestion of the acetylated BR1BR2 peptide revealed the presence of several pairs of peaks presumably corresponding to the unmodified and monoacetylated versions of the same peptides, as they differed by ~42 Da (Figure 4C, arrows). This point was confirmed for two peaks by MS/MS fragmentation (see Table 1). Figure 5 shows the fragmentation spectra obtained for one of these pairs of peptides. The presence of a peak at ~126.10 Da (an immonium ion of an acetylated lysine residue) in panel C, absent in panel B, indicated that a lysine residue was acetylated. Moreover, the molecular mass of all the peptides obtained fitted only when we assumed that the most N-terminal lysine of each of these peptides was acetylated (as shown in panel B). From these results, we conclude that lysine 325 is the only residue in the BR1BR2 peptide acetylated by PCAF. In agreement, all peptide pairs showing a mass increase of 42 Da included lysine 325 (see Table 1). We have no evidence of acetylation of any of the other lysine residues in this peptide.

On the basis of the observation that GAGADBD was diacetylated by PCAF (Figure 3), we similarly analyzed the BR3 peptide, containing region BR3. This peptide was monoacetylated [compare unmodified and modified spectra (panels A and B of Figure 6, respectively)]. Limited trypsin digestion of the acetylated BR3 peptide produced a series of pairs of peptides showing an increase of ~42 Da attributable to a single acetylation (Figure 6C, denoted by arrows). MS/MS fragmentation of one of these pairs (corresponding to 1280.8 and 1322.9 Da) resulted in several fragments whose molecular masses were consistent when assuming an acetylation at the lysine residue before the last one (Figure 7). Acetylated peptides containing this residue and the presence of an immonium ion peak of acetylated lysine at 126.12 Da support this assignment. In addition, none of these fragments were present in the spectrum for unmodified BR3 (compare panels A and B of Figure 7). In this case, two peptides were mapped and found to contain an acetylated lysine, after limited trypsin digestion or V8 digestion followed by MS/MS fragmentation, and gave consistent results. We then conclude that lysine 373 is a second acetylation site for PCAF in GAGADBD. We have no evidence of the acetylation of any of the other lysine residues in this peptide (see Table 2).

Functional Consequences of GAGADBD Acetylation. K325 and K373 are in basic regions BR1 and BR3, respectively, which were previously shown to help stabilize GAGADBD specific interaction with DNA. Thus, using an EMSA, we assayed the potential regulatory role that acetylation of these residues plays in the affinity of GAGA for DNA. Acetylated GAGADBD presented a significantly lower affinity for its cognate DNA than unmodified GAGADBD (Figure 8A). This result is possibly an underestimate of the true effect because we know that acetylation in vitro is not complete and results in a mixture of monoacetylated and, to a lesser extent, diacetylated GAGADBD, while a significant part of GAGADBD was unmodified (see Figure 3). To further study this contribution, K325 and K373 were mutated to glutamines, either individually or in combination, with the aim of mimicking a constitutive acetylated lysine residue and obtaining a

Table 1

peptide mass	position in BR1BR2 peptide (GAGA protein)	sequence	acetylation[e]
787.34[a]	1−7 (317−323)	STPKAKR	−
1018.38[a]	10−18 (326−334)	HPPGTEKPR	−
1217.48[b,c]	8−18 (324−334)	AKHPPGTEKPR	−
1259.48[b,c]	8−18 (324−334)	A**K**HPPGTEKPR	+
1373.56[b,c]	7−18 (323−334)	RAKHPPGTEKPR	−
1415.56[b,c]	7−18 (323−334)	RA**K**HPPGTEKPR	+
1460.58[a]	8−20 (324−336)	AKHPPGTEKPRSR	−
1502.58[a]	8−20 (324−336)	AKHPPGTEKPRSR	+
1572.66[a]	5−18 (321−334)	AKRAKHPPGTEKPR	−
1616.66[a]	7−20 (323−336)	RAKHPPGTEKPRSR	−
1658.66[a,d]	7−20 (323−336)	RAKHPPGTEKPRSR	+
1762.66[a,c]	8−23 (324−339)	AKHPPGTEKPRSRSQS	−
1804.66[a,c]	8−23 (324−339)	A**K**HPPGTEKPRSRSQS	+
1857.75[a,d]	5−20 (321−336)	AKRAKHPPGTEKPRSR	+
1918.74[a]	7−23 (323−339)	RAKHPPGTEKPRSRSQS	−
1960.75[a,c]	7−23 (323−339)	RA**K**HPPGTEKPRSRSQS	+
1985.83[a]	1−18 (317−334)	STPKAKRAKHPPGTEKPR	−
2027.84[a]	1−18 (317−334)	STPKAKRAKHPPGTEKPR	+
2117.84[a]	5−23 (321−339)	AKRAKHPPGTEKPRSRSQS	−
2228.94[a]	1−20 (317−336)	STPKAKRAKHPPGTEKPRSR	−
2270.94[a]	1−20 (317−336)	STPKAKRAKHPPGTEKPRSR	+

[a]Trypsin-digested peptide positions analyzed by MALDI-TOF. [b]Trypsin-digested peptide positions analyzed by MALDI-TOF MS/MS. [c]Arg-C-digested peptide positions analyzed by MALDI-TOF MS/MS (spectra not shown). [d]Arg-C-digested peptide positions analyzed by MALDI-TOF (spectra not shown). [e]Peptides with a mass increase (42 Da), consistent with the presence of an acetyl group, are marked with a plus. When acetylation was confirmed by MS/MS fragmentation, the precise lysine residue is shown in bold. All peptides that were subjected to MS/MS fragmentation showed K325 as the acetylated residue. All peptides with a 42 Da mass increase contained K325.

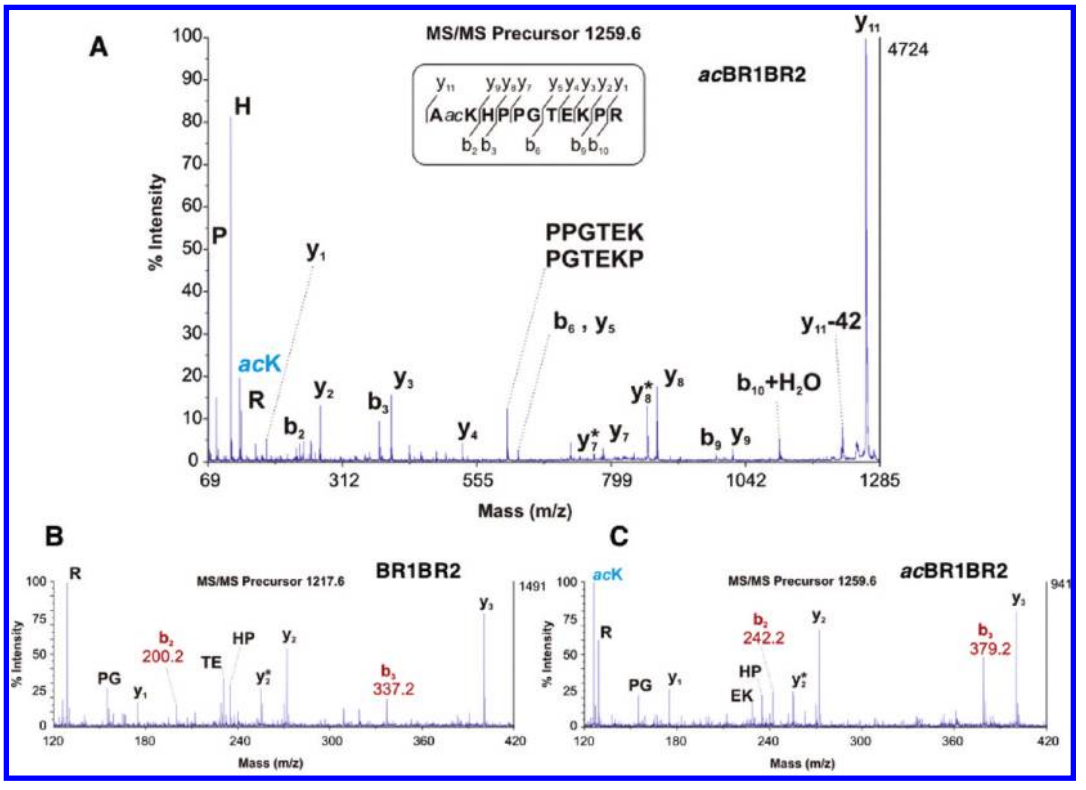

FIGURE 5: Identification of the acetylation site on BR1BR2. MS/MS spectra of the 1218/1259 pair of peptides corresponding to the nonacetylated (B) and acetylated (A and C) forms [(A) general view and (B and C) detailed view]. Peptide fragmentation generated a series of pair ions that unequivocally assign acetylation to Lys-325. Ions that have lost ammonia (−17 Da) are marked with an asterisk. Boxed sequences show the peptides analyzed and summarize the b and y ions detected. Immonium ions are labeled with the one-letter code for the corresponding amino acid. Internal fragmentation amino-acylium ions are shown by their sequences. Some internal fragments are not shown for the sake of clarity. *ac*K denotes the acetylated lysine immonium ion (*m*/*z* 126.1).

homogeneous sample, as previously described for other systems (*33*−*35*). Glutamine effectively mimics acetylated lysine in vivo, as exemplified by multiple Lys → Gln mutations that in p53 reproduce the strong inhibition of Mdm2-mediated ubiquitination elicited by the acetylation of those lysine residues (*34*). However, in our experiments, glutamine mutants did not reproduce the effect

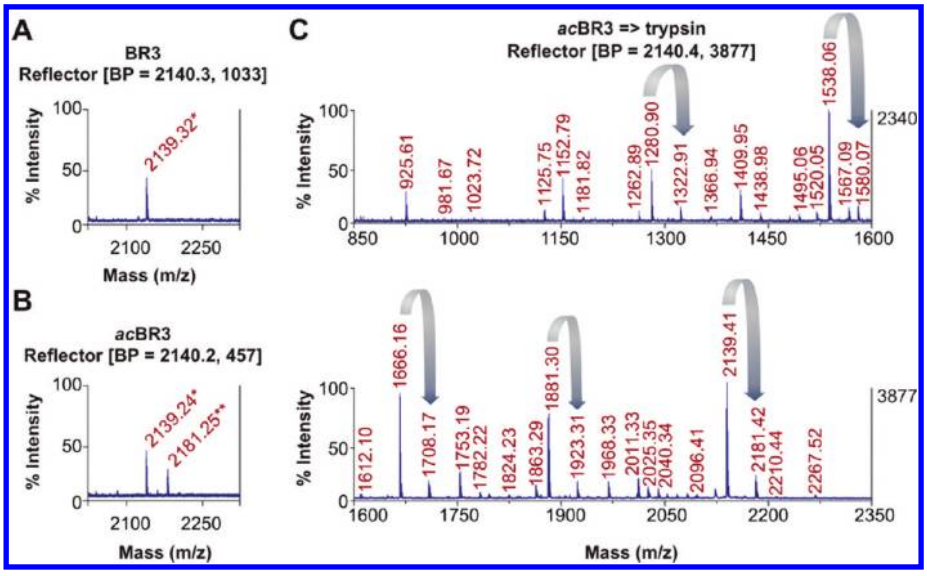

FIGURE 6: Basic region 3 is acetylated by HAT-PCAF at Lys373. Mass spectra of nonacetylated (labeled with anasterisk) (A) and of acetylated BR3 (labeled with two asterisks) (B). (C) Mass spectrum of acetylated BR3 digested with trypsin (see Materials and Methods). Arrows indicate several pairs of acetylated/nonacetylated peptides. The spectrum is split in two halves for the sake of convenience.

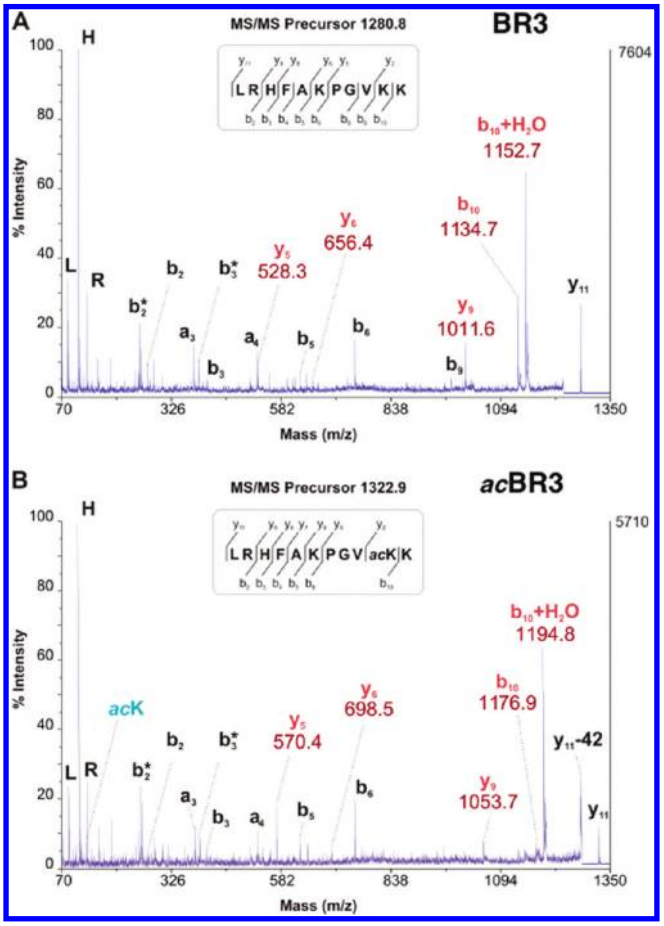

FIGURE 7: Identification of the acetylation site on BR3. MS/MS spectra of the −/− pair of peptides corresponding to the nonacetylated (A) and acetylated (B) forms. Peptide fragmentation generated a series of breaks that unequivocally assign acetylation to Lys-373. Boxed sequences show the peptides analyzed and summarize the b and y ions detected. Some internal fragments are not shown for the sake of clarity. *ac*K denotes the acetylated lysine immonium ion (*m*/*z* 126.1).

of the acetylated lysine residues because relative affinities for the cognate DNA were not significantly different, perhaps with the exception of the double mutant (Figure 8B). These point mutations were then used to assay the individual contribution of each of these two lysine residues to the acetylation of GAGADBD by PCAF, and their relative contributions to DNA affinity. When residues K325 and K373 were simultaneously mutated to nonacetylable glutamine residues, PCAF was largely unable to acetylate this GAGADBD mutant protein (Figure 8C, lane 4 in the left panel), thereby confirming our MS results. Also, K325 was the residue preferentially acetylated because in the K373Q mutant acetylation was comparable to that found in wild-type GAGADBD, while the

Table 2

peptide mass	position in BR3 peptide (GAGA protein)	sequence	acetylation[d]
925.61[a]	3−10 (366−373)	HFAKPGVK	+
1011.60[a]	3−11 (366−374)	HFAKPGVKK	−
1053.63[a]	3−11 (366−374)	HFAKPGVKK	+
1152.79[a]	1−10 (364−373)	LRHFAKPGVK	−
1194.73[a]	1−10 (364−373)	LRHFAKPGVK	+
1280.90[b]	1−11 (364−374)	LRHFAKPGVKK	−
1322.91[b]	1−11 (364−374)	LRHFAKPGV**K**K	+
1396.96[a]	3−14 (366−377)	HFAKPGVKKEKK	−
1409.83[c]	1−12 (364−375)	LRHFAKPGVKKE	−
1438.98[a]	3−14 (366−377)	HFAKPGVKKEKK	+
1451.83[c]	1−12 (364−375)	LRHFAKPGV**K**KE	+
1538.06[a]	1−13 (364−376)	LRHFAKPGVKKEK	−
1580.07[a]	1−13 (364−376)	LRHFAKPGVKKEK	+
1612.10[a]	3−16 (366−379)	HFAKPGVKKEKKSK	−
1666.16[a]	1−14 (364−377)	LRHFAKPGVKKEKK	−
1708.17[a]	1−14 (364−377)	LRHFAKPGVKKEKK	+
1881.30[a]	1−16 (364−379)	LRHFAKPGVKKEKKSK	−
1923.31[a]	1−16 (364−379)	LRHFAKPGVKKEKKSK	+

[a]Trypsin-digested peptide positions analyzed by MALDI-TOF. [b]Trypsin-digested peptide positions analyzed by MALDI-TOF MS/MS. [c]V8-digested peptide positions analyzed by MALDI-TOF MS/MS (spectra not shown). [d]Peptides with a mass increase (42 Da), consistent with the presence of an acetyl group, are marked with a plus. When acetylation was confirmed by MS/MS fragmentation, the precise lysine is shown in bold. All peptides that were subjected to MS/MS fragmentation show K373 as the acetylated residue. All peptides with a 42 Da mass increase contained K373.

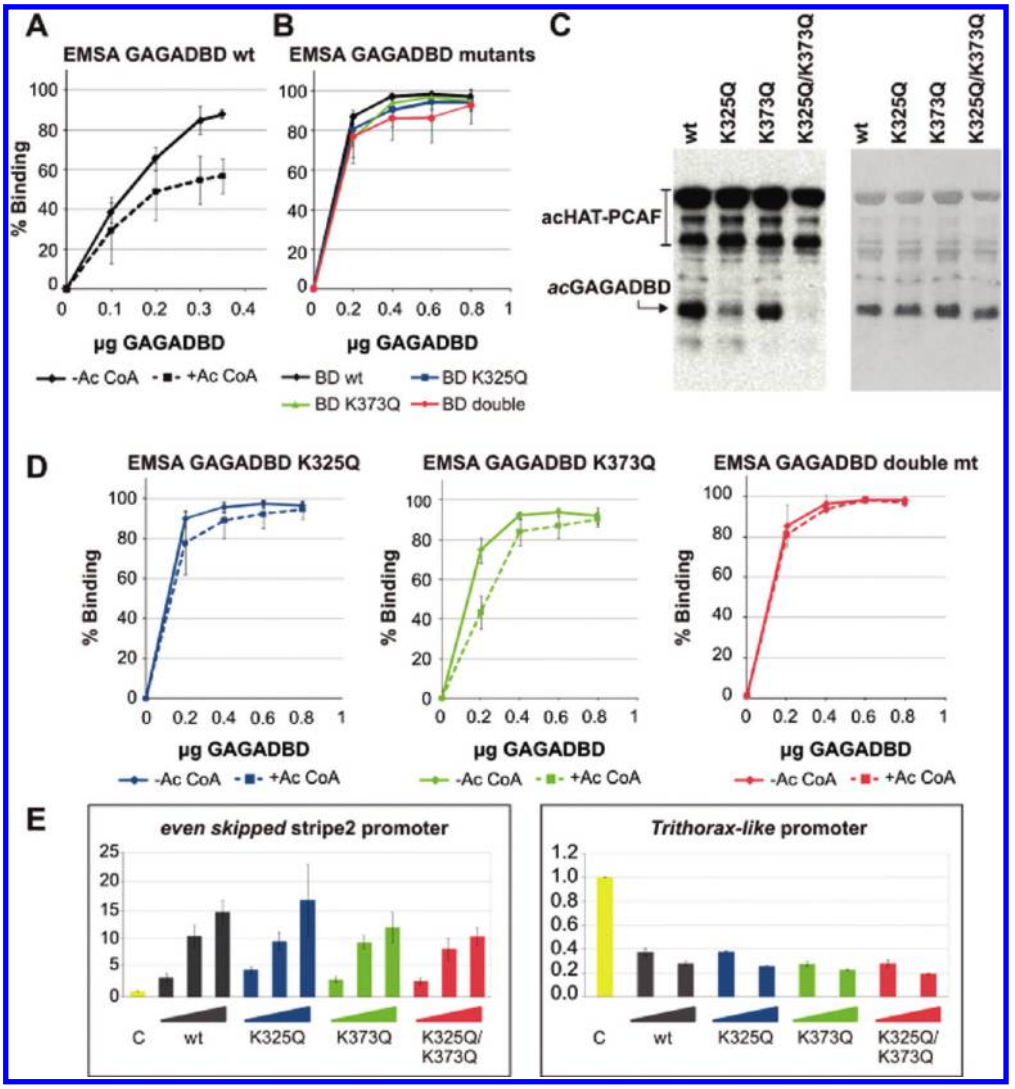

FIGURE 8: Acetylation of the BR1 and BR3 regions reduces GAGADBD DNA binding affinity. (A) Comparative plot of EMSA results obtained with nonacetylated (—) and acetylated (---) GAGADBD. (B) Comparative plot of EMSAs obtained with nonacetylated wild-type GAGADBD (black line) and mutants K325Q (blue line), K373Q (green line), and K325Q/K373Q (red line). (C) Comparative acetylation of wild-type GAGADBD and its mutants. Autoacetylated HAT/PCAF products are indicated with a bracket. The left panel shows the autoradiograph and the right panel Ponceau staining. (D) Comparative plots of EMSAs obtained with nonacetylated (—) and acetylated (---) GAGADBD for the K325Q, K373Q, and K325Q/K373Q mutants from left to right, respectively. (E) Transient transfection assays using increasing amounts of wild-type GAGADBD (gray bars) and mutants K325Q (blue bars), K373Q (green bars), and K325Q/K373Q (red bars). The left panel shows activation of even-skipped stripe 2 promoter; the right panel shows repression of Trithorax-like promoter. In all panels, mean results are shown and error bars depict the standard deviation of at least three independent assays.

mutant showed a much weaker acetylation (Figure 8C, left panel). The capacity of the acetylated and nonacetylated versions of these three mutant proteins to bind DNA was analyzed by an EMSA. Acetylation of the double point mutant had no effect (Figure 8D), a finding that is in agreement with its almost undetectable acetylation levels, as observed above (Figure 8C). In contrast, acetylation of the K373Q mutant had the largest effect on DNA affinity. These results suggest that individual acetylation of K325 has a considerable effect on DNA affinity. Furthermore, acetylation of the K325Q mutant also had a significant effect on DNA affinity, although it was less notable. We propose this slighter effect is the result of the lower acetylation efficiency of K373 by PCAF as shown above (Figure 8C). The observation that with larger protein amounts the reduction in affinity was not detected may reflect the partial acetylation of these mutant proteins (see spectra in Figures 3, 4, and 6).

Given that mutation of K325 and K373 to glutamines in GAGADBD constructs did not result in any significant change in DNA affinity, we analyzed the effect of these mutations on transcription, in the context of the full-length GAGA factor. Using a transient transfection assay, we found that these mutations did not show any defect in the activation of the even-skipped stripe 2 promoter, a well-known GAGA responding promoter (*36*), either individually or in combination with respect to wild-type GAGA factor (Figure 8E, left panel). Similarly, these mutations did not show any defect in the repression of the Trithorax-like promoter, the only promoter repressed by GAGA factor described to date (*19*) (Figure 8E, right panel). All these results indicate that while lysine residues K325 and K373 are directly involved in the modulation of binding of GAGA to DNA through acetylation, their role in stabilizing this interaction is of secondary importance.

Energetic Analysis of the GAGADBD−DNA Interaction. The K-to-Q mutation for mimicking lysine acetylation is controversial. Published results suggest that the final outcome of this mutation with respect to the activities assayed strongly

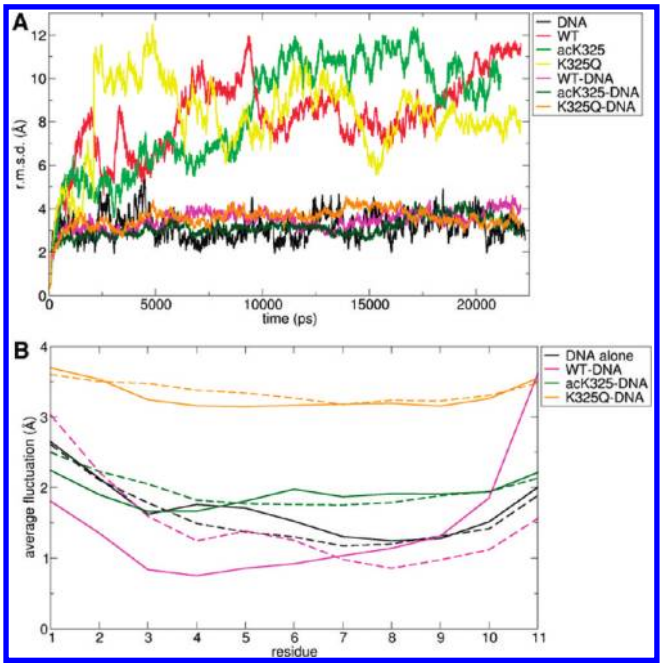

FIGURE 9: Molecular dynamics simulations of acK325 GAGADBD and K325Q GAGADBD. (A) Root-mean-square deviations (rmsd) of the structures from their starting states during the simulations as a function of time. Data for DNA alone are colored black, for GAGADBD only red (wild-type), green (acK325), and yellow (K325Q mutant), and for DNA−GAGADBD complexes magenta (DNA and wild type), dark green (DNA and acK325), and orange (DNA and K325Q). The profiles after the initial increase suggest the stability of the simulations conducted for the complexes. The higher rmsd values of the peptides are consistent with a poorly structured state when not bound to DNA. (B) Root-mean-square fluctuations per residue of the DNA, whether free (black) or bound to the studied GAGADBD peptides (colored as in panel A). For each complex, both DNA strands are depicted, one as a solid line and its complementary strand as a dashed line.

depends on the particular situation of the interaction tested (*33*−*35*, *37*).

To reconcile our results with the structural data, we analyzed the contribution of K325 acetylation and K325Q mutation to DNA interaction in more detail. To gain insight into the forces involved in the binding of DNA by GAGADBD, we conducted protein−DNA binding free energy calculations using the MM-PBSA method (*38*). MD simulations were conducted independently for the complexes and unbound molecules and were found to be stable. The rmsd values for the unbound peptides were ~3 times higher than those of their bound forms (Figure 9A). This observation is to be expected, because the DNA-binding domain of GAGA is likely to be fully ordered only upon binding to its substrate DNA. Table 3 summarizes the results of the MM-PBSA calculations. Our results indicate that the major contribution, after subtracting solvation energies, to the interaction of GAGADBD with its cognate DNA is from the van der Waals interaction energy. In both acK325 GAGADBD and K325Q GAGADBD, this contribution was decreased by ~9 kcal/mol. No other energy component offsets this loss of structural complementarity for the acetylated peptide. However, in the case of the K325Q mutant, this negative effect was offset by a better internal adaptation by a factor of ~18 kcal/mol, which was not observed in the acetylated structure (see ΔE_{int} in Table 3). Thus, the structure of the GAGA DNA binding domain appears to be less strained in this mutant than in the wild-type protein. The relaxation of the structure of the K325Q GAGADBD peptide

Table 3

parameter[a]	wild-type GAGADBD	acK325 GAGADBD	K325Q GAGADBD
ΔE_{ele}	−4547.9 ± 4.1	−4015.7 ± 4.9	−4149.8 ± 4.5
ΔE_{vdw}	−114.0 ± 1.1	−105.1 ± 1.1	−105.0 ± 1.0
ΔE_{int}	24.7 ± 1.9	22.8 ± 1.9	6.3 ± 1.9
ΔG_{PB}	4551.6 ± 3.9	4023.8 ± 4.6	4163.3 ± 4.2
ΔG_{np}	−18.8 ± 0.1	−15.3 ± 0.1	−15.9 ± 0.1
ΔG_{sol}	4532.9 ± 3.9	4008.5 ± 4.5	4147.7 ± 4.2
ΔG_{ele}	3.7 ± 1.4	8.1 ± 1.6	13.8 ± 1.5
ΔG_{tot}	−104.3 ± 1.9	−89.5 ± 2.0	−100.9 ± 1.9
$-T\Delta S$	69.2 ± 0.5	62.7 ± 0.5	62.7 ± 0.4
ΔG_{MMPBSA}	−33.3 ± 2.0	−25.0 ± 2.0	−36.4 ± 2.0

[a]Means and standard errors in kilocalories per mole. ΔE_{ele}, ΔE_{vdw}, and ΔE_{int} account for the electrostatic, van der Waals, and internal in vacuo binding energy contributions, respectively. ΔG_{PB} and ΔG_{np} represent the polar and nonpolar contributions to solvation, respectively. ΔG_{sol} denotes the sum of ΔG_{np} and ΔG_{PB}. ΔG_{ele} accounts for the addition of ΔE_{ele} and ΔG_{PB} and represents the net electrostatic contribution to binding. ΔG_{tot} stands for the sum of ΔG_{np} and ΔG_{PB}. ΔG_{tot} stands for the sum of the gas-phase and solvation free energies ($\Delta E_{ele} + \Delta E_{vdw} + \Delta E_{int} + \Delta G_{sol}$). $-T\Delta S$ accounts for the entropic balance. Finally, the theoretical free energy of binding at 300 K ($\Delta G_{tot} + E_{rot/trans} - T\Delta S$) is denoted ΔG_{MMPBSA}.

was achieved at the expense of the increased flexibility of the DNA structure. While wild-type GAGADBD stabilized the core of the bound DNA, the bulkier and uncharged peptides acK325 GAGADBD and, more dramatically, K325Q GAGADBD induced the opposite effect (Figure 9B). Consistent with this observation, entropy was slightly less unfavorable in the case of the neutralized and mutated DNA binding domains. Finally, the electrostatic contribution, which is slightly unfavorable for binding in all cases, was even more adverse for the complexes of DNA with the neutral acK325 and K325Q GAGADBD peptides. As a result of these balances, no significant effect was found for the mutated K325Q GAGADBD. In contrast, our simulations suggest that the free energy interaction between GAGADBD and DNA wass clearly affected (+8.3 kcal/mol) when K325 was acetylated, thus making its interaction weaker.

Similar expectations applied to the K373Q mutation because acetylation of this residue also reduced the affinity of GAGADBD for DNA. However, also in this case, no effect was observed. BR3 has been reported to be dispensable for the interaction of GAGADBD by an EMSA (*39*), and consequently, this region was not included in the published structure. Thus, no information about the position of K373 relative to DNA is available yet, and simulations are not possible.

DISCUSSION

Here we have shown that GAGA factor is acetylated in vivo. While modification by other acetylases is certainly possible, we have shown that acetylation by PCAF of K325 and K373, present in basic regions BR1 and BR3 of the GAGADBD, respectively, modulates the affinity of GAGA for DNA. In the published NMR structure, the model of interaction of the GAGADBD domain with its cognate DNA described K325 and R323 inserted deep into the minor groove of the DNA double helix, making contacts with several nitrogenated bases and with the sugar−phosphate backbone of the 5′ half of the GAGAG motif (*23*). These two residues account for the essential interaction with the DNA in the minor groove. Deleterious mutations at these two residues cannot be compensated by the presence of intact BR2 and BR3. In fact, deletion of the BR1

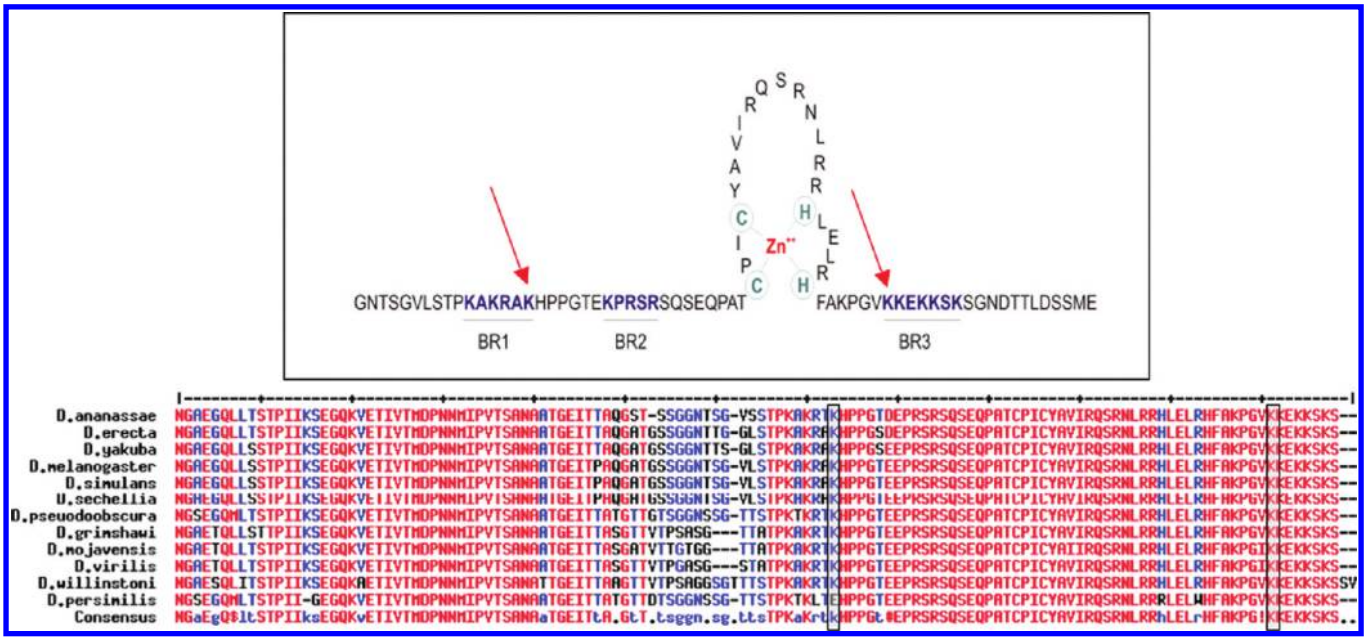

FIGURE 10: Scheme of GAGADBD. Arrows indicate PCAF-acetylable residues K325 and K373. Basic regions 1−3 (BR1−BR3, respectively) are indicated. A sequence alignment of the GAGADBD region performed on the 12 *Drosophila* species shows a high degree of conservation in general and total conservation of the K373 residue (below).

motif was shown to strongly affect the specificity and affinity of the interaction (*39*). Therefore, K325 acetylation was expected to affect these interactions, because of the possible steric hindrance generated by the acetyl group and also because of charge neutralization. Consequently, the K325Q mutant was expected to present a similar decrease in the affinity for DNA. However, this was not observed.

GAGADBD shows remarkable adaptability, for example, in its capacity to accommodate its specific interaction with its cognate DNA in a triple-stranded form with a minimal loss of affinity, because of the auxiliary interactions provided by basic regions BR1−BR3 surrounding the zinc finger domain (*40*). Thus, BRs remarkably contribute to the interaction of DBD with DNA and appear to be a key regulatory component.

We have shown that, compared to wild-type GAGADBD, neither the K325Q nor the K373Q mutant resulted in a decrease in the level of activation of a reporter gene or in an increase in the level of repression on another reporter gene, even when in combination. This finding clearly suggests that the loss of charge and the change in volume of the side chain do not affect GAGA functions. However, K325 and K373 are highly conserved across the 12 *Drosophila* species for which the genomic sequence is available for GAGA factor (Figure 10). We can estimate more than 60 million years of conservation of these residues after divergence between *Drosophila melanogaster* and *Drosophila virilis* (*41*). Paradoxically, our results indicate that the requirement for K325 and K373 in BR1 and BR3, respectively, is not strict because their mutation to glutamine did not affect DNA binding, transactivation activity, or repressive activity on the Trl promoter. We propose that while the contribution of these lysine residues to the stabilization of the GAGADBD−DNA interaction can be afforded by other residues, their conservation is due to their potential to regulate the affinity for its cognate DNA through PTMs, in particular acetylation. In this respect, it is remarkable that while BR3 is dispensable for binding of GAGADBD to DNA, acetylation of K373 reduces its affinity. This observation clearly indicates that BR3 is more relevant for regulatory purposes than for stabilizing the interaction of the GAGADBD zinc finger with DNA. Also, acetylation of K325 in BR1 affects the affinity of GAGADBD for DNA. On the basis of our results, we cannot estimate whether acetylation of K325 is more relevant than that of K373, or vice versa, because we observed only partial acetylation in our samples. However, the use of mutated GAGADBDs allowed us to unequivocally conclude that both acetylations result in a reduction in the affinity of DNA for this domain. Given that we have repeatedly observed that acetylation occurs preferentially on K325 (Figure 8C, for example), the contribution of acetylated K373 could be remarkable.

Because the lysine residues that we identified as becoming acetylated are common to $GAGA_{519}$ and $GAGA_{581}$ isoforms, their acetylation might be a mechanism used to downregulate GAGA factor functions in a general manner. This would contrast with CKII-mediated phosphorylation, which, although affecting the affinity of GAGADBD for DNA in a similar manner, modifes only the $GAGA_{519}$ isoform (*4*).

GAGA factor is expressed ubiquitously in the fly, and very little is known about its regulation. GAGA factor depletion and overexpression experiments have recently revealed phenotypic defects that appear to be much more restricted than expected, thereby suggesting that GAGA functions differ depending on the tissues involved (*42*). It is tempting to speculate that PTMs are used to preferentially direct GAGA to a subset of specific targets and/or functions. In this regard, an accumulation of acetylated peptides in multiprotein complexes involved in several nuclear functions along with evidence supporting a regulatory role of their acetylation has been reported in vivo in human cells (*43*). Thus, acetylation and phosphorylation, either individually or in combination, may affect binding of GAGA factor to weaker, nonconsensus, sites more dramatically than binding to higher-affinity sites. This might result in displacement of GAGA factor from the weakest sites on promoters and eventually affect and/or redirect activity. Moreover, this modulation may be wider and also more tunable. The oligomeric nature of GAGA factor combined with its binding to clustered sites, in association with

the PTMs described, will give rise to a broad range of sites for which GAGA could display differential affinities and allow fine-tuned regulation of GAGA functions that can be easily and rapidly reversed. The complexity of the 2D gel pattern observed suggests the presence of other PTMs and indicates even more complexity in the regulation of GAGA, a transcription factor essential for the fly.

ACKNOWLEDGMENT

We thank F. Azorín, M. Martínez-Balbás, and all the members of our lab for discussion and advice. We also acknowledge A. Vera for expert technical assistance, C. S. Verma for thoughtful discussions about the MM-PBSA analyses, and Tanya Yates (IRB) for editorial assistance.

REFERENCES

1. Strahl, B. D., and Allis, D. (2000) The language of covalent histone modifications. *Nature 403*, 41–45.
2. Carter, S., and Vousden, K. H. (2009) Modifications of p53: Competing for the lysines. *Curr. Opin. Genet. Dev. 19*, 18–24.
3. Kruse, J.-P., and Gu, W. (2009) Modes of p53 regulation. *Cell 137*, 609–622.
4. Bonet, C., Fernández, I., Aran, X., Bernués, J., Giralt, E., and Azorín, F. (2005) The GAGA protein of *Drosophila* is phoshorylated by CK2. *J. Mol. Biol. 351*, 562–572.
5. Farkas, G., Gausz, J., Galloni, M., Reuter, G., Gyurkovics, H., and Karch, F. (1994) The *Trithorax-like* gene encodes the *Drosophila* GAGA factor. *Nature 371*, 806–808.
6. Granok, H., Leibovitch, B. A., Shaffer, C. D., and Elgin, S. C. R. (1995) Ga-ga over GAGA factor. *Curr. Biol. 5*, 238–241.
7. Lehman, M. (2004) Anything else but GAGA: A nonhistone protein complex reshapes chromatin structure. *Trends Genet. 20*, 15–22.
8. Adkins, N. L., Hagerman, T. A., and Georgel, P. (2006) GAGA protein: A multi-faceted transcription factor. *Biochem. Cell Biol. 84*, 559–567.
9. Jackson, S. P., and Tjian, R. (1988) O-Glycosylation of eukaryotic transcription factors: Implications for mechanisms of transcriptional regulation. *Cell 55*, 125–133.
10. Espinás, M. L., Jiménez-García, E., Vaquero, A., Canudas, S., Bernués, J., and Azorín, F. (1999) The N-terminal POZ-domain of GAGA mediates the formation of oligomers that bind DNA with high affinity and specificity. *J. Biol. Chem. 274*, 16461–16469.
11. Vaquero, A., Scher, M., Lee, D., Erdjument-Bromage, H., Tempst, P., and Reinberg, D. (2004) HUman SirT1 interacts with histone H1 and promotes formation of facultative heterochromatin. *Mol. Cell 16*, 93–105.
12. Reid, J. L., Bannister, A. J., Zegerman, P., Martínez-Balbás, M. A., and Kouzarides, T. (1998) E1A directly binds and regulates the P/CAF acetyltransferase. *EMBO J. 17*, 4469–4477.
13. Valls, E., Blanco-García, N., Aquizu, N., Piedra, D., Estarás, C., de la Cruz, X., and Martínez-Balbás, M. A. (2007) Involvement of chromatin and histone deacetylation in SV40 T antigen transcription regulation. *Nucleic Acids Res. 35*, 1958–1968.
14. Martínez-Balbás, A., Bannister, A. J., Martin, K., Haus-Seuffert, P., Meisterernst, M., and Kouzarides, T. (1998) The acetyltransferase activity of CBP stimulates transcription. *EMBO J. 17*, 2776–2893.
15. Brehm, A., Miska, E. A., McCance, D. J., Reid, J. L., Bannister, A. J., and Kouzarides, T. (1998) Retinoblastoma protein recruits histone deacetylase to repress transcription. *Nature 391*, 597–601.
16. Landry, J., Sutton, A., Tafrov, S. T., Heller, R. C., Stebbins, J., Pillus, L., and Sternglanz, R. (2000) The silencing protein SIR2 and its homologous are NAD-dependent protein deacetylases. *Proc. Natl. Acad. Sci. U.S.A. 97*, 5807–5811.
17. Biggin, M. D., and Tjian, R. (1988) Transcription factors that activate the *Ultrabithorax* promoter in developmentally staged extracts. *Cell 53*, 699–711.
18. Espinás, M. L., Jiménez-García, E., Martínez-Balbás, A., and Azorín, F. (1996) Formation of triple-stranded DNA at $d(GA\cdot TC)_n$ sequences prevents nucleosome assembly and is hindered by nucleosomes. *J. Biol. Chem. 271*, 31807–31812.
19. Kosoy, A., Pagans, S., Espinás, M. L., Azorín, F., and Bernués, J. (2002) GAGA factor down regulates its own promoter. *J. Biol. Chem. 277*, 42280–42288.
20. Vaquero, A., Espinás, M. L., Azorín, F., and Bernués, J. (2000) Functional mapping of the GAGA factor assigns its transcriptional activity to the C-terminal glutamine-rich domain. *J. Biol. Chem. 275*, 19461–19468.
21. Cornell, W. D., Cieplak, P., Bayly, C. I., Gould, I. R., Merz, K. M., Ferguson, D. M., Spellmeyer, D. C., Fox, T., Caldwell, J. W., and Kollman, P. A. (1995) A Second Generation Force Field for the Simulation of Proteins, Nucleic Acids, and Organic Molecules. *J. Am. Chem. Soc. 117*, 5179–5197.
22. Case, D. A., Darden, T. A., Cheatham, T. E., III, Simmerling, C. L., Wang, J., Duke, R. E., Luo, R., Merz, K. M., Pearlman, D. A., Crowley, M., Walker, R. C., Zhang, W., Wang, B., Hayik, S., Roitberg, A., Seabra, G., Wong, K. F., Paesani, F., Wu, X., Brozell, S., Tsui, V., Gohlke, H., Yang, L., Tang, C., Mongan, J., Hornak, V., Cui, G., Beroza, P., Mathews, D. H., Schafmeister, C., Ross, W. S., and Kollman, P. A. (2006) AMBER 9, University of California, San Francisco.
23. Omichinski, J. G., Pedone, P. V., Felsenfeld, G., Gronenborn, A. M., and Clore, G. M. (1997) The solution structure of a specific GAGA factor-DNA complex reveals a modular binding mode. *Nat. Struct. Biol. 4*, 122–132.
24. Bayly, C. I., Cieplak, P., Cornell, W., and Kollman, P. A. (1993) A well-behaved electrostatic potential based method using charge restraints for deriving atomic charges: the RESP model. *J. Phys. Chem. 97*, 10269–10280.
25. Pigache, A., Cieplak, P., and Dupradeau, F. (2004) Automatic and highly reproducible RESP and ESP charge derivation: Application to the development of programs RED and X RED. 227th ACS National Meeting, Anaheim, CA.
26. Cieplak, P., Cornell, W., Bayly, C., and Kollman, P. (1995) Application of the multimolecule and multiconformational RESP methodology to biopolymers: Charge derivation for DNA, RNA and proteins. *J. Comput. Chem. 16*, 1357–1377.
27. Wang, J., Wang, W., Kollman, P. A., and Case, D. A. (2006) Automatic atom type and bond type perception in molecular mechanical calculations. *J. Mol. Graphics Modell. 25*, 247–260.
28. Ryde, U. (1995) Molecular dynamics simulations of alcohol dehydrogenase with a four- or five-coordinate catalytic zinc ion. *Proteins 21*, 40–56.
29. Darden, T., York, D., and Pedersen, L. (1993) Particle mesh Ewald: An N* log (N) method for computing Ewald sums. *J. Chem. Phys. 98*, 10089–10092.
30. Ryckaert, J., Ciccotti, G., and Berendsen, H. J. C. (1977) Numerical integration of the Cartesian equations of motion of a system with constraints: Molecular dynamics of n-alkanes. *J. Comput. Phys. 23*, 327–341.
31. Sitkoff, D., Sharp, K. A., and Honig, B. (1994) Accurate Calculation of Hydration Free Energies Using Macroscopic Solvent Models. *J. Phys. Chem. 98*, 1978–1988.
32. Carré, C., Szymczak, D., Pidoux, J., and Antoniewski, C. (2005) The histone H3 acetylase dGCN5 is a key player in *Drosophila melanogaster* metamorphosis. *Mol. Cell. Biol. 25*, 8228–8238.
33. Hecht, A., Laroche, T., Strahl-Bolsinger, S., Gasser, S. M., and Grunstein, M. (1995) Histone H3 and H4 N-termini interact with SIR3 and SIR4 proteins: A molecular model for the formation of heterochromatin in yeast. *Cell 80*, 583–592.
34. Li, M., Luo, J., Brooks, C. L., and Gu, W. (2002) Acetylation of p53 inhibits its ubiquitination by Mdm2. *J. Biol. Chem. 277*, 50607–50611.
35. Matsuzaki, H., Daitoku, H., Hatta, M., Aoyama, H., Yoshimochi, K., and Fukamizu, A. (2005) Acetylation of Foxo1 alters its DNA-binding ability and sensitivity to phosphorylation. *Proc. Natl. Acad. Sci. U.S.A. 102*, 11278–11283.
36. Pagans, S., Ortiz-Lombardía, M., Espinás, M. L., Bernués, J., and Azorín, F. (2002) The *Drosophila* transcription factor *tramtrack* interacts with GAGA and represses GAGA-mediated activation. *Nucleic Acids Res. 30*, 4406–4413.
37. Kasten, M., Szerlong, H., Erdjument-Bromage, H., Tempst, P., Werner, M., and Cairns, B. R. (2004) Tandem bromodomains in the chromatin remodeler RSC recognize acetylated histone H3 Lys14. *EMBO J. 23*, 1348–1359.
38. Kollman, P. A., Massova, I., Reyes, C., Kuhn, B., Huo, S., Chong, L., Lee, M., Lee, T., Duan, Y., Wang, W., Donini, O., Cieplak, P., Srinivasan, J., Case, D. A., and Cheatham, T. E., III (2000) Calculating structures and free energies of complex molecules: Combining molecular mechanics and continuum models. *Acc. Chem. Res. 33*, 889–897.
39. Pedone, P. V., Ghirlando, R., Clore, G. M., Gronenborn, A. M., Felsenfeld, G., and Omichinski, J. G. (1996) The single cys_2-his_2 zinc finger domain of the GAGA protein flanked by basic residues is

sufficient for high affinity specific DNA binding. *Proc. Natl. Acad. Sci. U.S.A. 93*, 2822–2826.
40. Jiménez-García, E., Vaquero, A., Espinás, M. L., Soliva, R., Orozco, M., Bernués, J., and Azorín, F. (1998) The GAGA factor of *Drosophila* binds triple-stranded DNA. *J. Biol. Chem. 273*, 24640–24648.
41. Beverley, S. M., and Wilson, A. C. (1984) Molecular evolution in *Drosophila* and the higher Diptera II. A time scale for fly evolution. *J. Mol. Evol. 21*, 1–13.
42. Bernués, J., Piñeyro, D., and Kosoy, A. (2007) General, negative feedback mechanism for regulation of *Trithorax-like* gene expression *in vivo*: New roles for GAGA factor in flies. *Nucleic Acids Res. 35*, 7150–7159.
43. Choudhary, C., Kumar, C., Gnad, F., Nielsen, M. L., Rehman, M., Walther, T. C., Olsen, J. V., and Mann, M. (2009) Lysine acetylation targets protein complexes and co-regulates major cellular functions. *Science 325*, 834–840.